Search for Third Generation Vector Leptoquarks in $p\overline{p}$ Collisions at $\sqrt{s} = 1.96\,\mathrm{TeV}$

T. Aaltonen,[23] A. Abulencia,[24] J. Adelman,[13] T. Affolder,[10] T. Akimoto,[55] M.G. Albrow,[17] S. Amerio,[43] D. Amidei,[35] A. Anastassov,[52] K. Anikeev,[17] A. Annovi,[19] J. Antos,[14] M. Aoki,[55] G. Apollinari,[17] T. Arisawa,[57] A. Artikov,[15] W. Ashmanskas,[17] A. Attal,[3] A. Aurisano,[53] F. Azfar,[42] P. Azzi-Bacchetta,[43] P. Azzurri,[46] N. Bacchetta,[43] W. Badgett,[17] A. Barbaro-Galtieri,[29] V.E. Barnes,[48] B.A. Barnett,[25] S. Baroiant,[7] V. Bartsch,[31] G. Bauer,[33] P.-H. Beauchemin,[34] F. Bedeschi,[46] S. Behari,[25] G. Bellettini,[46] J. Bellinger,[59] A. Belloni,[33] D. Benjamin,[16] A. Beretvas,[17] J. Beringer,[29] T. Berry,[30] A. Bhatti,[50] M. Binkley,[17] D. Bisello,[43] I. Bizjak,[31] R.E. Blair,[2] C. Blocker,[6] B. Blumenfeld,[25] A. Bocci,[16] A. Bodek,[49] V. Boisvert,[49] G. Bolla,[48] A. Bolshov,[33] D. Bortoletto,[48] J. Boudreau,[47] A. Boveia,[10] B. Brau,[10] L. Brigliadori,[5] C. Bromberg,[36] E. Brubaker,[13] J. Budagov,[15] H.S. Budd,[49] S. Budd,[24] K. Burkett,[17] G. Busetto,[43] P. Bussey,[21] A. Buzatu,[34] K. L. Byrum,[2] S. Cabrera,[q,16] M. Campanelli,[20] M. Campbell,[35] F. Canelli,[17] A. Canepa,[45] S. Carrillo,[i,18] D. Carlsmith,[59] R. Carosi,[46] S. Carron,[34] B. Casal,[11] M. Casarsa,[54] A. Castro,[5] P. Catastini,[46] D. Cauz,[54] M. Cavalli-Sforza,[3] A. Cerri,[29] L. Cerrito,[m,31] S.H. Chang,[28] Y.C. Chen,[1] M. Chertok,[7] G. Chiarelli,[46] G. Chlachidze,[17] F. Chlebana,[17] I. Cho,[28] K. Cho,[28] D. Chokheli,[15] J.P. Chou,[22] G. Choudalakis,[33] S.H. Chuang,[52] K. Chung,[12] W.H. Chung,[59] Y.S. Chung,[49] M. Cilijak,[46] C.I. Ciobanu,[24] M.A. Ciocci,[46] A. Clark,[20] D. Clark,[6] M. Coca,[16] G. Compostella,[43] M.E. Convery,[50] J. Conway,[7] B. Cooper,[31] K. Copic,[35] M. Cordelli,[19] G. Cortiana,[43] F. Crescioli,[46] C. Cuenca Almenar,[q,7] J. Cuevas,[l,11] R. Culbertson,[17] J.C. Cully,[35] S. DaRonco,[43] M. Datta,[17] S. D'Auria,[21] T. Davies,[21] D. Dagenhart,[17] P. de Barbaro,[49] S. De Cecco,[51] A. Deisher,[29] G. De Lentdecker,[c,49] G. De Lorenzo,[3] M. Dell'Orso,[46] F. Delli Paoli,[43] L. Demortier,[50] J. Deng,[16] M. Deninno,[5] D. De Pedis,[51] P.F. Derwent,[17] G.P. Di Giovanni,[44] C. Dionisi,[51] B. Di Ruzza,[54] J.R. Dittmann,[4] M. D'Onofrio,[3] C. Dörr,[26] S. Donati,[46] P. Dong,[8] J. Donini,[43] T. Dorigo,[43] S. Dube,[52] J. Efron,[39] R. Erbacher,[7] D. Errede,[24] S. Errede,[24] R. Eusebi,[17] H.C. Fang,[29] S. Farrington,[30] I. Fedorko,[46] W.T. Fedorko,[13] R.G. Feild,[60] M. Feindt,[26] J.P. Fernandez,[32] R. Field,[18] G. Flanagan,[48] R. Forrest,[7] S. Forrester,[7] M. Franklin,[22] J.C. Freeman,[29] I. Furic,[13] M. Gallinaro,[50] J. Galyardt,[12] J.E. Garcia,[46] F. Garberson,[10] A.F. Garfinkel,[48] C. Gay,[60] H. Gerberich,[24] D. Gerdes,[35] S. Giagu,[51] P. Giannetti,[46] K. Gibson,[47] J.L. Gimmell,[49] C. Ginsburg,[17] N. Giokaris,[a,15] M. Giordani,[54] P. Giromini,[19] M. Giunta,[46] G. Giurgiu,[25] V. Glagolev,[15] D. Glenzinski,[17] M. Gold,[37] N. Goldschmidt,[18] J. Goldstein,[b,42] A. Golossanov,[17] G. Gomez,[11] G. Gomez-Ceballos,[33] M. Goncharov,[53] O. González,[32] I. Gorelov,[37] A.T. Goshaw,[16] K. Goulianos,[50] A. Gresele,[43] S. Grinstein,[22] C. Grosso-Pilcher,[13] R.C. Group,[17] U. Grundler,[24] J. Guimaraes da Costa,[22] Z. Gunay-Unalan,[36] C. Haber,[29] K. Hahn,[33] S.R. Hahn,[17] E. Halkiadakis,[52] A. Hamilton,[20] B.-Y. Han,[49] J.Y. Han,[49] R. Handler,[59] F. Happacher,[19] K. Hara,[55] D. Hare,[52] M. Hare,[56] S. Harper,[42] R.F. Harr,[58] R.M. Harris,[17] M. Hartz,[47] K. Hatakeyama,[50] J. Hauser,[8] C. Hays,[42] M. Heck,[26] A. Heijboer,[45] B. Heinemann,[29] J. Heinrich,[45] C. Henderson,[33] M. Herndon,[59] J. Heuser,[26] D. Hidas,[16] C.S. Hill,[b,10] D. Hirschbuehl,[26] A. Hocker,[17] A. Holloway,[22] S. Hou,[1] M. Houlden,[30] S.-C. Hsu,[9] B.T. Huffman,[42] R.E. Hughes,[39] U. Husemann,[60] J. Huston,[36] J. Incandela,[10] G. Introzzi,[46] M. Iori,[51] A. Ivanov,[7] B. Iyutin,[33] E. James,[17] D. Jang,[52] B. Jayatilaka,[16] D. Jeans,[51] E.J. Jeon,[28] S. Jindariani,[18] W. Johnson,[7] M. Jones,[48] K.K. Joo,[28] S.Y. Jun,[12] J.E. Jung,[28] T.R. Junk,[24] T. Kamon,[53] P.E. Karchin,[58] Y. Kato,[41] Y. Kemp,[26] R. Kephart,[17] U. Kerzel,[26] V. Khotilovich,[53] B. Kilminster,[39] D.H. Kim,[28] H.S. Kim,[28] J.E. Kim,[28] M.J. Kim,[17] S.B. Kim,[28] S.H. Kim,[55] Y.K. Kim,[13] N. Kimura,[55] L. Kirsch,[6] S. Klimenko,[18] M. Klute,[33] B. Knuteson,[33] B.R. Ko,[16] K. Kondo,[57] D.J. Kong,[28] J. Konigsberg,[18] A. Korytov,[18] A.V. Kotwal,[16] A.C. Kraan,[45] J. Kraus,[24] M. Kreps,[26] J. Kroll,[45] N. Krumnack,[4] M. Kruse,[16] V. Krutelyov,[10] T. Kubo,[55] S. E. Kuhlmann,[2] T. Kuhr,[26] N.P. Kulkarni,[58] Y. Kusakabe,[57] S. Kwang,[13] A.T. Laasanen,[48] S. Lai,[34] S. Lami,[46] S. Lammel,[17] M. Lancaster,[31] R.L. Lander,[7] K. Lannon,[39] A. Lath,[52] G. Latino,[46] I. Lazzizzera,[43] T. LeCompte,[2] J. Lee,[49] J. Lee,[28] Y.J. Lee,[28] S.W. Lee,[o,53] R. Lefèvre,[20] N. Leonardo,[33] S. Leone,[46] S. Levy,[13] J.D. Lewis,[17] C. Lin,[60] C.S. Lin,[17] M. Lindgren,[17] E. Lipeles,[9] A. Lister,[7] D.O. Litvintsev,[17] T. Liu,[17] N.S. Lockyer,[45] A. Loginov,[60] M. Loreti,[43] R.-S. Lu,[1] D. Lucchesi,[43] P. Lujan,[29] P. Lukens,[17] G. Lungu,[18] L. Lyons,[42] J. Lys,[29] R. Lysak,[14] E. Lytken,[48] P. Mack,[26] D. MacQueen,[34] R. Madrak,[17] K. Maeshima,[17] K. Makhoul,[33] T. Maki,[23] P. Maksimovic,[25] S. Malde,[42] S. Malik,[31] G. Manca,[30] A. Manousakis,[a,15] F. Margaroli,[5] R. Marginean,[17] C. Marino,[26] C.P. Marino,[24] A. Martin,[60] M. Martin,[25] V. Martin,[g,21] M. Martínez,[3] R. Martínez-Ballarín,[32] T. Maruyama,[55] P. Mastrandrea,[51] T. Masubuchi,[55] H. Matsunaga,[55] M.E. Mattson,[58] R. Mazini,[34] P. Mazzanti,[5] K.S. McFarland,[49] P. McIntyre,[53] R. McNulty,[f,30] A. Mehta,[30] P. Mehtala,[23] S. Menzemer,[h,11] A. Menzione,[46] P. Merkel,[48] C. Mesropian,[50] A. Messina,[36] T. Miao,[17] N. Miladinovic,[6] J. Miles,[33] R. Miller,[36] C. Mills,[10] M. Milnik,[26] A. Mitra,[1] G. Mitselmakher,[18] A. Miyamoto,[27] S. Moed,[20] N. Moggi,[5] B. Mohr,[8] C.S. Moon,[28]

R. Moore,[17] M. Morello,[46] P. Movilla Fernandez,[29] J. Mülmenstädt,[29] A. Mukherjee,[17] Th. Muller,[26] R. Mumford,[25]
P. Murat,[17] M. Mussini,[5] J. Nachtman,[17] A. Nagano,[55] J. Naganoma,[57] K. Nakamura,[55] I. Nakano,[40] A. Napier,[56]
V. Necula,[16] C. Neu,[45] M.S. Neubauer,[9] J. Nielsen[n],[29] L. Nodulman,[2] O. Norniella,[3] E. Nurse,[31] S.H. Oh,[16]
Y.D. Oh,[28] I. Oksuzian,[18] T. Okusawa,[41] R. Oldeman,[30] R. Orava,[23] K. Osterberg,[23] C. Pagliarone,[46]
E. Palencia,[11] V. Papadimitriou,[17] A. Papaikonomou,[26] A.A. Paramonov,[13] B. Parks,[39] S. Pashapour,[34]
J. Patrick,[17] G. Pauletta,[54] M. Paulini,[12] C. Paus,[33] D.E. Pellett,[7] A. Penzo,[54] T.J. Phillips,[16] G. Piacentino,[46]
J. Piedra,[44] L. Pinera,[18] K. Pitts,[24] C. Plager,[8] L. Pondrom,[59] X. Portell,[3] O. Poukhov,[15] N. Pounder,[42]
F. Prakoshyn,[15] A. Pronko,[17] J. Proudfoot,[2] F. Ptohos[e],[19] G. Punzi,[46] J. Pursley,[25] J. Rademacker[b],[42]
A. Rahaman,[47] V. Ramakrishnan,[59] N. Ranjan,[48] I. Redondo,[32] B. Reisert,[17] V. Rekovic,[37] P. Renton,[42]
M. Rescigno,[51] S. Richter,[26] F. Rimondi,[5] L. Ristori,[46] A. Robson,[21] T. Rodrigo,[11] E. Rogers,[24] S. Rolli,[56]
R. Roser,[17] M. Rossi,[54] R. Rossin,[10] P. Roy,[34] A. Ruiz,[11] J. Russ,[12] V. Rusu,[13] H. Saarikko,[23] A. Safonov,[53]
W.K. Sakumoto,[49] G. Salamanna,[51] O. Saltó,[3] L. Santi,[54] S. Sarkar,[51] L. Sartori,[46] K. Sato,[17] P. Savard,[34]
A. Savoy-Navarro,[44] T. Scheidle,[26] P. Schlabach,[17] E.E. Schmidt,[17] M.P. Schmidt,[60] M. Schmitt,[38] T. Schwarz,[7]
L. Scodellaro,[11] A.L. Scott,[10] A. Scribano,[46] F. Scuri,[46] A. Sedov,[48] S. Seidel,[37] Y. Seiya,[41] A. Semenov,[15]
L. Sexton-Kennedy,[17] A. Sfyrla,[20] S.Z. Shalhout,[58] M.D. Shapiro,[29] T. Shears,[30] P.F. Shepard,[47] D. Sherman,[22]
M. Shimojima[k],[55] M. Shochet,[13] Y. Shon,[59] I. Shreyber,[20] A. Sidoti,[46] P. Sinervo,[34] A. Sisakyan,[15] A.J. Slaughter,[17]
J. Slaunwhite,[39] K. Sliwa,[56] J.R. Smith,[7] F.D. Snider,[17] R. Snihur,[34] M. Soderberg,[35] A. Soha,[7] S. Somalwar,[52]
V. Sorin,[36] J. Spalding,[17] F. Spinella,[46] T. Spreitzer,[34] P. Squillacioti,[46] M. Stanitzki,[60] A. Staveris-Polykalas,[46]
R. St. Denis,[21] B. Stelzer,[8] O. Stelzer-Chilton,[42] D. Stentz,[38] J. Strologas,[37] D. Stuart,[10] J.S. Suh,[28] A. Sukhanov,[18]
H. Sun,[56] I. Suslov,[15] T. Suzuki,[55] A. Taffard[p],[24] R. Takashima,[40] Y. Takeuchi,[55] R. Tanaka,[40] M. Tecchio,[35]
P.K. Teng,[1] K. Terashi,[50] J. Thom[d],[17] A.S. Thompson,[21] E. Thomson,[45] P. Tipton,[60] V. Tiwari,[12] S. Tkaczyk,[17]
D. Toback,[53] S. Tokar,[14] K. Tollefson,[36] T. Tomura,[55] D. Tonelli,[46] S. Torre,[19] D. Torretta,[17] S. Tourneur,[44]
W. Trischuk,[34] S. Tsuno,[40] Y. Tu,[45] N. Turini,[46] F. Ukegawa,[55] S. Uozumi,[55] S. Vallecorsa,[20] N. van Remortel,[23]
A. Varganov,[35] E. Vataga,[37] F. Vazquez[i],[18] G. Velev,[17] C. Vellidis[a],[46] G. Veramendi,[24] V. Veszpremi,[48] M. Vidal,[32]
R. Vidal,[17] I. Vila,[11] R. Vilar,[11] T. Vine,[31] M. Vogel,[37] I. Vollrath,[34] I. Volobouev[o],[29] G. Volpi,[46] F. Würthwein,[9]
P. Wagner,[53] R.G. Wagner,[2] R.L. Wagner,[17] J. Wagner,[26] W. Wagner,[26] R. Wallny,[8] S.M. Wang,[1] A. Warburton,[34]
D. Waters,[31] M. Weinberger,[53] W.C. Wester III,[17] B. Whitehouse,[56] D. Whiteson[p],[45] A.B. Wicklund,[2]
E. Wicklund,[17] G. Williams,[34] H.H. Williams,[45] P. Wilson,[17] B.L. Winer,[39] P. Wittich[d],[17] S. Wolbers,[17]
C. Wolfe,[13] T. Wright,[35] X. Wu,[20] S.M. Wynne,[30] A. Yagil,[9] K. Yamamoto,[41] J. Yamaoka,[52] T. Yamashita,[40]
C. Yang,[60] U.K. Yang[j],[13] Y.C. Yang,[28] W.M. Yao,[29] G.P. Yeh,[17] J. Yoh,[17] K. Yorita,[13] T. Yoshida,[41] G.B. Yu,[49]
I. Yu,[28] S.S. Yu,[17] J.C. Yun,[17] L. Zanello,[51] A. Zanetti,[54] I. Zaw,[22] X. Zhang,[24] J. Zhou,[52] and S. Zucchelli[5]

(CDF Collaboration[*])

[1]Institute of Physics, Academia Sinica, Taipei, Taiwan 11529, Republic of China
[2]Argonne National Laboratory, Argonne, Illinois 60439
[3]Institut de Fisica d'Altes Energies, Universitat Autonoma de Barcelona, E-08193, Bellaterra (Barcelona), Spain
[4]Baylor University, Waco, Texas 76798
[5]Istituto Nazionale di Fisica Nucleare, University of Bologna, I-40127 Bologna, Italy
[6]Brandeis University, Waltham, Massachusetts 02254
[7]University of California, Davis, Davis, California 95616
[8]University of California, Los Angeles, Los Angeles, California 90024
[9]University of California, San Diego, La Jolla, California 92093
[10]University of California, Santa Barbara, Santa Barbara, California 93106
[11]Instituto de Fisica de Cantabria, CSIC-University of Cantabria, 39005 Santander, Spain
[12]Carnegie Mellon University, Pittsburgh, PA 15213
[13]Enrico Fermi Institute, University of Chicago, Chicago, Illinois 60637
[14]Comenius University, 842 48 Bratislava, Slovakia; Institute of Experimental Physics, 040 01 Kosice, Slovakia
[15]Joint Institute for Nuclear Research, RU-141980 Dubna, Russia
[16]Duke University, Durham, North Carolina 27708
[17]Fermi National Accelerator Laboratory, Batavia, Illinois 60510
[18]University of Florida, Gainesville, Florida 32611
[19]Laboratori Nazionali di Frascati, Istituto Nazionale di Fisica Nucleare, I-00044 Frascati, Italy
[20]University of Geneva, CH-1211 Geneva 4, Switzerland
[21]Glasgow University, Glasgow G12 8QQ, United Kingdom
[22]Harvard University, Cambridge, Massachusetts 02138
[23]Division of High Energy Physics, Department of Physics,
University of Helsinki and Helsinki Institute of Physics, FIN-00014, Helsinki, Finland

[24] *University of Illinois, Urbana, Illinois 61801*
[25] *The Johns Hopkins University, Baltimore, Maryland 21218*
[26] *Institut für Experimentelle Kernphysik, Universität Karlsruhe, 76128 Karlsruhe, Germany*
[27] *High Energy Accelerator Research Organization (KEK), Tsukuba, Ibaraki 305, Japan*
[28] *Center for High Energy Physics: Kyungpook National University,*
Taegu 702-701, Korea; Seoul National University, Seoul 151-742,
Korea; SungKyunKwan University, Suwon 440-746, Korea
[29] *Ernest Orlando Lawrence Berkeley National Laboratory, Berkeley, California 94720*
[30] *University of Liverpool, Liverpool L69 7ZE, United Kingdom*
[31] *University College London, London WC1E 6BT, United Kingdom*
[32] *Centro de Investigaciones Energeticas Medioambientales y Tecnologicas, E-28040 Madrid, Spain*
[33] *Massachusetts Institute of Technology, Cambridge, Massachusetts 02139*
[34] *Institute of Particle Physics: McGill University, Montréal,*
Canada H3A 2T8; and University of Toronto, Toronto, Canada M5S 1A7
[35] *University of Michigan, Ann Arbor, Michigan 48109*
[36] *Michigan State University, East Lansing, Michigan 48824*
[37] *University of New Mexico, Albuquerque, New Mexico 87131*
[38] *Northwestern University, Evanston, Illinois 60208*
[39] *The Ohio State University, Columbus, Ohio 43210*
[40] *Okayama University, Okayama 700-8530, Japan*
[41] *Osaka City University, Osaka 588, Japan*
[42] *University of Oxford, Oxford OX1 3RH, United Kingdom*
[43] *University of Padova, Istituto Nazionale di Fisica Nucleare,*
Sezione di Padova-Trento, I-35131 Padova, Italy
[44] *LPNHE, Universite Pierre et Marie Curie/IN2P3-CNRS, UMR7585, Paris, F-75252 France*
[45] *University of Pennsylvania, Philadelphia, Pennsylvania 19104*
[46] *Istituto Nazionale di Fisica Nucleare Pisa, Universities of Pisa,*
Siena and Scuola Normale Superiore, I-56127 Pisa, Italy
[47] *University of Pittsburgh, Pittsburgh, Pennsylvania 15260*
[48] *Purdue University, West Lafayette, Indiana 47907*
[49] *University of Rochester, Rochester, New York 14627*
[50] *The Rockefeller University, New York, New York 10021*
[51] *Istituto Nazionale di Fisica Nucleare, Sezione di Roma 1,*
University of Rome "La Sapienza," I-00185 Roma, Italy
[52] *Rutgers University, Piscataway, New Jersey 08855*
[53] *Texas A&M University, College Station, Texas 77843*
[54] *Istituto Nazionale di Fisica Nucleare, University of Trieste/ Udine, Italy*
[55] *University of Tsukuba, Tsukuba, Ibaraki 305, Japan*
[56] *Tufts University, Medford, Massachusetts 02155*
[57] *Waseda University, Tokyo 169, Japan*
[58] *Wayne State University, Detroit, Michigan 48201*
[59] *University of Wisconsin, Madison, Wisconsin 53706*
[60] *Yale University, New Haven, Connecticut 06520*
(Dated: June 19, 2007)

We describe a search for a third generation vector leptoquark ($VLQ3$) that decays to a b quark and tau lepton using the CDF II detector and $322\,\mathrm{pb}^{-1}$ of integrated luminosity from the Fermilab Tevatron. Vector leptoquarks have been proposed in many extensions of the standard model (SM). Observing a number of events in agreement with SM expectations, assuming Yang-Mills (minimal) couplings, we obtain the most stringent upper limit on the $VLQ3$ pair production cross section of $344\,\mathrm{fb}$ ($493\,\mathrm{fb}$) and lower limit on the $VLQ3$ mass of $317\,\mathrm{GeV}/c^2$ ($251\,\mathrm{GeV}/c^2$) at 95% C.L.

PACS numbers: 14.80.-j, 13.85.Rm

*With visitors from [a]University of Athens, 15784 Athens, Greece, [b]University of Bristol, Bristol BS8 1TL, United Kingdom, [c]University Libre de Bruxelles, B-1050 Brussels, Belgium, [d]Cornell University, Ithaca, NY 14853, [e]University of Cyprus, Nicosia CY-1678, Cyprus, [f]University College Dublin, Dublin 4, Ireland, [g]University of Edinburgh, Edinburgh EH9 3JZ, United King-

dom, [h]University of Heidelberg, D-69120 Heidelberg, Germany, [i]Universidad Iberoamericana, Mexico D.F., Mexico, [j]University of Manchester, Manchester M13 9PL, England, [k]Nagasaki Institute of Applied Science, Nagasaki, Japan, [l]University de Oviedo, E-33007 Oviedo, Spain, [m]University of London, Queen Mary College, London, E1 4NS, England, [n]University of California Santa

Despite its extraordinary success, the standard model (SM) of elementary particles has structural deficiencies. The parallels between the families of quarks and leptons suggest a possible link between these two sectors at higher mass scales. Leptoquarks, therefore, have been proposed as fractionally-charged color-triplet bosons carrying both lepton and baryon quantum numbers. Leptoquarks appear in a wide range of theories, including SU(5) grand unification [1], superstrings [2], SU(4) Pati-Salam [3], and compositeness models [4]; direct searches for leptoquarks at hadron colliders probe the parameter space of some of these models.

The various leptoquark states are classified according to the quantum numbers of SM gauge group interactions [5]. At the Tevatron collider, these states would be predominately pair produced through quark anti-quark annihilation. In general, larger cross sections, and thus better search sensitivities, are predicted for vector (spin 1) than for scalar leptoquarks [6].

We search for third generation vector leptoquark ($VLQ3$) pair production, and assume each $VLQ3$ decays promptly to a b quark and a tau lepton. As the trilinear and quartic couplings between vector leptoquarks and gluons can have model-dependent "anomalous" contributions, we examine two scenarios: one with Yang-Mills couplings, where vector leptoquarks are fundamental gauge bosons of an extended gauge group, and the other with minimal anomalous couplings [6, 7]. Previous $VLQ3$ searches have been carried out in experiments at $p\overline{p}$, e^+e^-, and ep colliders [8, 9, 10, 11]. Our new results substantially extend the reach beyond the previous limits.

The results reported in this Letter are obtained from data corresponding to $322\,\mathrm{pb}^{-1}$ of integrated luminosity collected between March 2002 and August 2004 by the CDF II detector [12], operating at the Tevatron $p\overline{p}$ collider. Detector components relevant to this search are described briefly here. The charged particle tracking volume, which is inside a uniform 1.4 T magnetic field, includes a multi-layer silicon microstrip detector system and an open-cell drift chamber (COT) that provide position, momentum, and charge information in the range $|\eta| < 1.0$ [13]. Outside the solenoid, electromagnetic (EM) and hadronic calorimeters are arranged in a projective tower geometry to measure electron, photon, and jet energies. A set of strip and wire chambers (CES) is embedded in the EM calorimeter, at the depth where the longitudinal development of EM showers is expected to be maximal, and provides information used for the identification of electron candidates and reconstruction

Cruz, Santa Cruz, CA 95064, [o]Texas Tech University, Lubbock, TX 79409, [p]University of California, Irvine, Irvine, CA 92697, [q]IFIC(CSIC-Universitat de Valencia), 46071 Valencia, Spain.

of π^0 candidates that decay through $\pi^0 \to \gamma\gamma$. Outside the calorimeters, drift chambers and scintillators provide muon candidate identification in the range $|\eta| < 1.0$.

This search assumes a branching ratio $\mathcal{B}(VLQ3 \to b\tau) = 1$, and considers a signature where the decay products of the $VLQ3$ pair, $\tau^+\tau^-b\overline{b}$, yield two jets from the b quarks, an electron or muon from a leptonically decaying tau, and a hadronically decaying tau (τ_h). We do not attempt to identify the jets as originating from b quarks, as we find this would degrade the search sensitivity. A three-level trigger system selects events with lepton candidates and charged tracks [14]. These events are then classified as $e\tau_h$ or $\mu\tau_h$ based on the flavor of the leptonic tau decay.

Selected events are required to contain at least one well-identified electron (muon) candidate that passes fully through the fiducial volume of the COT, with transverse energy (momentum) $E_T > 10\,\mathrm{GeV}$ ($p_T > 10\,\mathrm{GeV}/c$) [13]. To reduce the background due to multijet quantum chromodynamics (QCD) events, an isolation requirement is imposed upon the electron or muon candidate. Specifically, the sum of the p_T of all additional tracks within a cone in $\eta - \phi$ space of $\Delta R < 0.4$ around the track direction of the candidate is required to be less than $2\,\mathrm{GeV}/c$, where $\Delta R \equiv \sqrt{\Delta\eta^2 + \Delta\phi^2}$.

Hadronic tau candidates are formed by matching narrow clusters of calorimeter towers with tracks. The procedure is described briefly here and in detail elsewhere [15]. A cluster is seeded by a tower with $E_T > 6\,\mathrm{GeV}$. The highest p_T track with $p_T > 6\,\mathrm{GeV}/c$ that points to the cluster is defined as the seed track. Other tracks are added if they are within an angle of 0.05 to 0.17 radians from the seed track, where the angle depends on the total cluster energy. Tau candidates with one or three tracks are considered. We reconstruct π^0 candidates as single narrow strip and wire clusters in the CES, and include them as part of the τ_h candidate if they are within 0.17 radians of the seed track and have $E_T > 1\,\mathrm{GeV}$. The τ_h candidates are required to have $|\eta| < 1.0$ and $E_T > 15\,\mathrm{GeV}$. To reduce instances where a jet is misidentified as a τ_h, we place requirements on the mass formed by constituent tracks, $m_{\mathrm{trk}} < 1.8\,\mathrm{GeV}/c^2$, and the mass formed from tracks and π^0 mesons within the tau candidate, $m_{\mathrm{trk}+\pi^0} < 2.5\,\mathrm{GeV}/c^2$. To better discriminate hadronic taus from electrons, we require the ratio of E_T deposited in the hadronic calorimeter to the sum of the magnitudes of the transverse momenta of the tau tracks to be greater than 0.1. To obtain isolated τ_h candidates, we require that the region outside the track selection cone, but inside a cone of 0.52 radians from the seed track, contains no tracks with $p_T > 1\,\mathrm{GeV}/c$. In addition, the region outside the π^0 inclusion cone, but inside a cone of 0.52 radians from the seed track, is required to contain less than $0.6\,\mathrm{GeV}$ of summed E_T due to π^0 candidates.

To ensure efficient event reconstruction, the electron

or muon candidate (ℓ) direction must be separated from the tau candidate direction by $\Delta R(\tau_h, \ell) > 0.7$. Jet candidates, with $E_T > 15\,\text{GeV}$, are identified in the region $|\eta| < 2.4$ and are required to be separated from the lepton candidates by $\Delta R(\ell/\tau_h, \text{jet}) > 0.8$.

There are a number of SM processes which can mimic the $VLQ3$ signal. The first category consists of background processes which contain a real $e\tau_h$ or $\mu\tau_h$ plus two jets. The primary processes are $Z^0/\gamma^* \to \tau\tau$ plus two jets, and $t\bar{t} \to WbWb$, where one W yields a hadronic tau via $W \to \tau\nu_\tau$, the other W similarly yields an electron (muon) or leptonically decaying tau, and the two b quarks give jets.

The second category of backgrounds consists of those that include misidentified final state particles. These include $t\bar{t} \to WbWb$, where a jet from a hadronic W decay can be misidentified as an electron (muon). The processes $t\bar{t} \to WbWb$, $Z^0/\gamma^* \to e^+e^-$ plus jets, and $Z^0/\gamma^* \to \mu^+\mu^-$ plus jets also contribute as backgrounds when an electron (muon) or jet is misidentified as the τ_h. Events with W plus jets can pass the selection if one of at least three jets is misidentified as the τ_h. Contributions from diboson channels (WW, WZ, and ZZ) plus jets are negligible. The above contributions and their uncertainties are estimated using PYTHIA [16] Monte Carlo simulation and GEANT [17] CDF II detector simulation. Background from multi-jet QCD can contribute when jets from quarks are misidentified as an electron (muon) or τ_h. Photon plus jets background enters when high-p_T photons convert within the detector and at least one of the resulting electrons appears as a primary electron candidate, while a jet is misidentified as the τ_h. Contributions from both of these sources are estimated directly from the data, using methods described elsewhere [15].

Further event selection reduces the backgrounds. Backgrounds associated with misidentification are reduced by approximately one-half through a requirement of oppositely charged electron (muon) and τ_h candidates, where the charge of the τ_h candidate is defined as the sum of the charges of all constituent tracks. Events consistent with photon conversions and cosmic rays are removed. To reduce contributions from Z boson production, events are rejected if $76 < m(\ell, X) < 106\,\text{GeV}/c^2$, where X can be the tau candidate or a second electron candidate in the $e\tau_h$ channel, or a second muon candidate in the $\mu\tau_h$ channel. We require $\not{E}_T > 10\,\text{GeV}$, where $\not{E}_T$ is the magnitude of the missing transverse energy [13]. This requirement reduces backgrounds from $Z^0/\gamma^* \to \tau^+\tau^-$ and multi-jet QCD processes and is nearly 100% efficient for the signal process. We define H_T as the scalar sum of electron (muon) candidate E_T, tau candidate E_T, event $\not{E}_T$, and the transverse energies of the two highest E_T jet candidates. The requirements on H_T are given below. The final selection requirement is that the event must contain two or more jets.

To simulate $VLQ3$ pair production and decay [18], we have added the production and decay processes to the GRACE [19] matrix element event generator, which calculates amplitudes, and to the GR@PPA [20] interface, which speeds up computations of the interactions of the primary hadrons. In addition to providing the theoretical cross section, these programs yield events that are processed through TAUOLA [21] to simulate tau decays, PYTHIA [16] to simulate parton showering, fragmentation, and additional particle decays, and GEANT [17] for the full CDF II detector simulation. For the first time, this framework includes helicity amplitudes for the full matrix element at tree level and propagation of helicity information from the leptoquarks to the tau decay products. We use the parton distribution functions (PDFs) CTEQ5L [22] and renormalization energy scale $Q^2 = m_{VLQ3}{}^2$.

We determine total selection efficiencies, including factors for triggering, geometrical and kinematic acceptance, particle candidate identification and isolation, and background suppression criteria. The total efficiencies, averaged between the $e\tau_h$ and $\mu\tau_h$ channels, range from about 2.2% (1.4%) to about 6.1% (5.9%) for Yang-Mills (minimal) couplings over the mass range $160\,\text{GeV}/c^2$ to $400\,\text{GeV}/c^2$. For the example of $m_{VLQ3} = 320\,\text{GeV}/c^2$ and Yang-Mills couplings, the efficiencies for the $e\tau_h$ and $\mu\tau_h$ channels are $(6.0 \pm 0.1)\%$ and $(6.1 \pm 0.1)\%$ respectively.

We define two signal regions. In addition, three sideband control regions in the plane of the number of jets (N_{jets}) versus H_T are used to verify the expected composition of the backgrounds and the distributions for kinematic quantities. The primary signal region (SR$_\text{A}$) has $N_{\text{jets}} \geq 2$ and $H_T > 400\,\text{GeV}$, and is sensitive to the highest mass leptoquarks. The secondary signal region (SR$_\text{B}$) has $N_{\text{jets}} \geq 2$ and $250 < H_T < 400\,\text{GeV}$, and adds sensitivity to lower $VLQ3$ masses (down to the previous mass limits). The three control regions are called CR0J, CR1J, and CR2J, where 0J, 1J, or 2J specifies the number of jets (0, 1, or ≥ 2). Regions CR0J and CR1J include the H_T range $H_T > 80\,\text{GeV}$, while region CR2J is restricted to $80 < H_T < 250\,\text{GeV}$. Table I shows the expected background contributions in the control and signal regions, as well as the number of events observed in all regions. The signal regions are examined only after an *a priori* optimization of the H_T ranges that maximizes signal sensitivity. Control region CR1J in the $\mu\tau_h$ channel contains the largest difference between the expected and observed number of events, with a difference of 1.9 sigma. Figure 1 shows the H_T distributions for the $e\tau_h$ and $\mu\tau_h$ channels, and includes the control region CR2J and the two signal regions.

The dominant sources of systematic uncertainties on the signal efficiencies are the amount of initial state radiation (ISR) and final state radiation (FSR), the tau identification, and the isolation requirements. The ISR and FSR uncertainties, as evaluated by varying the amount of ISR and FSR in simulation, are each approximately 3.7% of the selection efficiency. The tau identification

TABLE I: Numbers of events observed in data and estimates for the total background, for the $e\tau_h$ and $\mu\tau_h$ channels, in the control regions (CR0J, CR1J, CR2J) and signal regions (SR$_B$, SR$_A$). For the backgrounds, the statistical uncertainty is given first, followed by the systematic uncertainty.

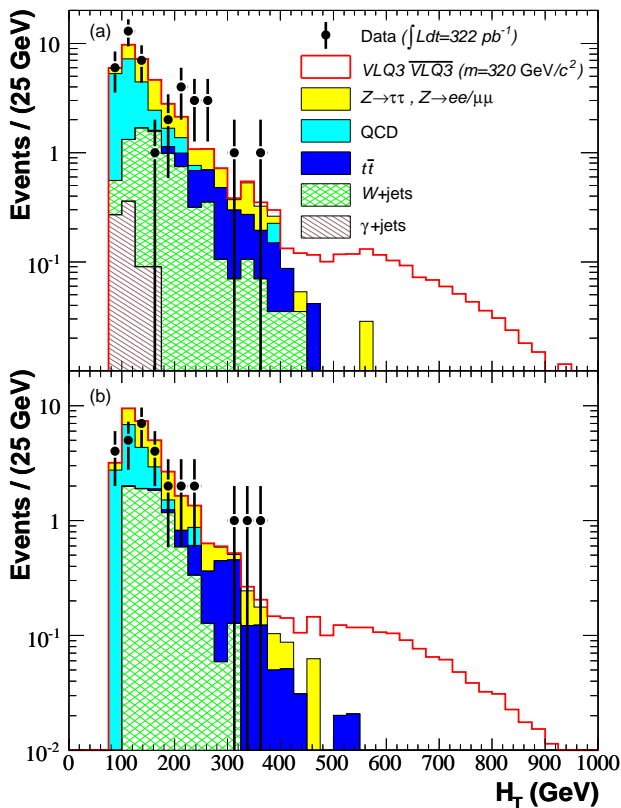| | $e\tau_h$ | | $\mu\tau_h$ | |
	Data	Background	Data	Background
CR0J	129	$122.1 \pm 2.1 \pm 11.3$	129	$147.1 \pm 2.6 \pm 12.3$
CR1J	110	$109.2 \pm 2.3 \pm 9.3$	79	$100.5 \pm 2.5 \pm 6.7$
CR2J	36	$33.4 \pm 1.4 \pm 4.8$	26	$30.6 \pm 1.6 \pm 3.8$
SR$_B$	5	$3.3 \pm 0.3 \pm 0.5$	3	$2.2 \pm 0.3 \pm 0.3$
SR$_A$	0	$0.3 \pm 0.1 \pm 0.1$	0	$0.2 \pm 0.1 \pm 0.1$

FIG. 1: Distributions of H_T for the (a) $e\tau_h$ channel and (b) $\mu\tau_h$ channel, including one of the control regions used for validation ($80 < H_T < 250\,\text{GeV}$), and the regions used for the search ($H_T > 250\,\text{GeV}$). The individual background contributions are shown, as is a hypothetical signal with mass $m_{VLQ3} = 320\,\text{GeV}/c^2$, normalized to the data sample size.

systematic uncertainty, as measured using methods described elsewhere [15], is 3.0% of the selection efficiency and is primarily due to uncertainties in the response of the hadronic calorimeter to charged tracks and uncertainties in the track reconstruction efficiency. Uncertainty in simulating the effect of the lepton isolation require-

ment is evaluated by comparing the efficiency of this isolation requirement in data and simulation. This yields a 3.0% uncertainty on the selection efficiency. Additional sources of systematic uncertainty on the signal efficiency are the choices of the PDFs and the jet energy scale, as well as smaller contributions from the acceptance criteria, the electron (muon) identification, and the $\not{E}_T$ simulation. The total systematic uncertainty on signal efficiency ranges from 10.5% (10.4%) for the $e\tau_h$ ($\mu\tau_h$) channel, for a $VLQ3$ with mass $m_{VLQ3} = 160\,\text{GeV}/c^2$, down to 7.0% (7.4%) for $m_{VLQ3} = 400\,\text{GeV}/c^2$. The systematic uncertainties on the theoretical prediction of the $VLQ3$ pair production cross section arise from the choices of PDFs and renormalization scale Q^2. These two contributions are combined in quadrature.

A likelihood function is constructed using a Poisson probability distribution of the expected rates of signal plus backgrounds and observed number of events in each channel and signal region. For each $VLQ3$ mass, the expected signal rates are functions of the $VLQ3$ pair production cross section. The expected signal rates also include factors for the branching ratios of leptonic and hadronic tau decays, luminosity, and full selection efficiencies. Systematic uncertainties, including 6% due to the luminosity measurement (not included in Table I), are incorporated into the fit. We apply Gaussian probabilities for the uncertainties on the background estimates, and account for correlations among different sources of systematic uncertainties. To set cross section limits for each mass, we integrate the likelihood distribution over all parameters except the cross section, and then integrate as a function of cross section from zero up to the cross section where the integral reaches 0.95.

The results are shown in Fig. 2, as a function of $VLQ3$ mass, along with the theoretical predictions. For a $VLQ3$ with Yang-Mills couplings, at 95% confidence level (C.L.), the upper limit on the cross section is $\sigma < 344\,\text{fb}$, assuming $\mathcal{B}(VLQ3 \to b\tau) = 1$, and the lower limit on the mass is $m_{VLQ3} > 317\,\text{GeV}/c^2$. With theoretical uncertainties included on the predicted cross section, the results are $\sigma < 360\,\text{fb}$ and $m_{VLQ3} > 294\,\text{GeV}/c^2$. For the minimal couplings model, the upper limit on the cross section is $\sigma < 493\,\text{fb}$ and the lower limit on the mass is $m_{VLQ3} > 251\,\text{GeV}/c^2$. With theoretical uncertainties included on the predicted cross section, the results are $\sigma < 610\,\text{fb}$ and $m_{VLQ3} > 223\,\text{GeV}/c^2$. The mass limits are approximately $80 - 90\,\text{GeV}/c^2$ higher than those of previous comparable results [8, 9].

Using $322\,\text{pb}^{-1}$ of luminosity at CDF II, we have searched for $VLQ3$ pair production and subsequent decay to two tau leptons and two jets. We observe no excess of events beyond the expected SM processes and set the most stringent limits to date on the $VLQ3$ mass and pair production cross section in the context of two coupling scenarios.
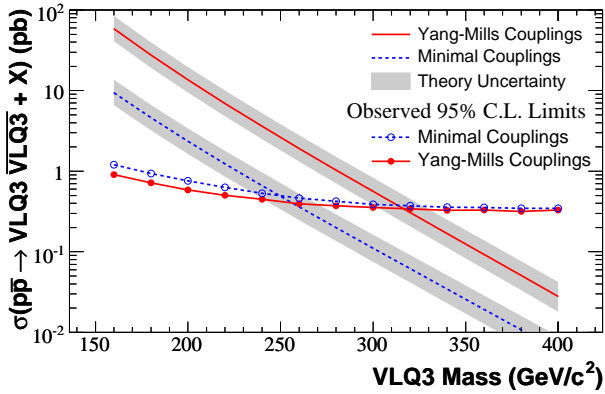
FIG. 2: The 95% C.L. upper limits for *VLQ3* pair production versus mass. Also shown are the theoretical predictions using the simulation described in the text, with bands for uncertainties due to the choices of PDFs and Q^2.

[1] H. Georgi and S.L. Glashow, Phys. Rev. Lett. **32**, 438 (1974).
[2] J.L. Hewett and T.G. Rizzo, Phys. Rep. **183**, 193 (1989).
[3] J.C. Pati and A. Salam, Phys. Rev. D **10**, 275 (1974).
[4] B. Schrempp and F. Schrempp, Phys. Lett. B **153**, 101 (1985).
[5] W. Buchmuller, R. Ruckl, and D. Wyler, Phys. Lett. B **191**, 442 (1987).
[6] J.L. Hewett *et al.*, in Proceedings of the Workshop on Physics at Current Accelerators and Supercolliders, Argonne National Lab, Argonne Accel. Phys. 539-546 (1993).
[7] J. Blumlein, E. Boos, and A. Kryukov, Z. Phys. C **76**, 137 (1997).
[8] F. Abe *et al.* (CDF Collaboration), Phys. Rev. Lett. **78**, 2906 (1997).
[9] B. Abbott *et al.* (DØ Collaboration), Phys. Rev. Lett. **81**, 38 (1998).
[10] G. Abbiendi *et al.* (OPAL Collaboration), Eur. Phys. J. C **31**, 281 (2003).
[11] S. Aid *et al.* (H1 Collaboration), Phys. Lett. B **369**, 173 (1996).
[12] D. Acosta *et al.* (CDF Collaboration), Phys. Rev. D **71**, 032001 (2005).
[13] We use a cylindrical coordinate system with the z axis along the beam axis, polar angle θ, azimuthal angle ϕ, and pseudorapidity $\eta \equiv -\ln\tan(\theta/2)$. We define $p_T \equiv p\sin\theta$ and $E_T \equiv E\sin\theta$, where p is the momentum measured by the tracking chambers and E is the energy measured by the calorimeters. The missing transverse energy is defined by $\vec{\rlap{/}E}_T = -\sum_i E_T^i \hat{n}_i$, where $i =$ calorimeter tower number with $|\eta| < 3.6$ and $\hat{n}_i$ is a unit vector perpendicular to the beam axis and pointing at the ith calorimeter tower. We also define $\rlap{/}E_T = |\vec{\rlap{/}E}_T|$.
[14] A. Anastassov *et al.*, Nucl. Instrum. Methods Phys. Res. A **518**, 609 (2004).
[15] A. Abulencia *et al.* (CDF Collaboration), Phys. Rev. D. **75**, 092004 (2007).
[16] T. Sjostrand *et al.*, Comput. Phys. Commun. **76**, 361 (1993); TP 01-21, LU (2001), hep-ph/0108264. We use version 6.2.
[17] R. Brun and F. Carminati, CERN Programming Library Long Writeup **W5013** (1993).
[18] B. C. Allanach *et al.*, "Les Houches 'Physics at TeV colliders 2005' Beyond the standard model working group: Summary report," page 104 (2006), hep-ph/0602198.
[19] Minami-Tateya Group, GRACE manual, KEK Report 92-19 (1993); F. Yuasa *et al.*, Prog. Theor. Phys. Suppl. **138**, 18 (2000).
[20] S. Tsuno, T. Kaneko, Y. Kurihara, S. Odaka, and K. Kato, Comput. Phys. Commun. **175**, 665 (2006).
[21] S. Jadach, J. H. Kuhn, and Z. Was, Comput. Phys. Commun. **64**, 275 (1990).
[22] J. Pumplin *et al.*, J. High Energy Phys. **0207**, 012 (2002).